Aluminum sampling by Chelex, titanium dioxide and zirconium oxide DGT: Influence of pH on accumulation behaviors

Juliette Rougerie, Rémy Buzier, Stéphane Simon, Gilles Guibaud

1   **Aluminum sampling by Chelex, Titanium dioxide and Zirconium oxide DGT: Influence of pH**

2   **on accumulation behaviors**

3   Authors: Rougerie Juliette, Buzier Rémy*, Simon Stéphane, Guibaud Gilles.

4   Université de Limoges, PEIRENE-Equipe DIQeau - URA IRSTEA, 123 Avenue Albert Thomas, Limoges

5   Cedex, 87060, France

6   *Corresponding author: remy.buzier@unilim.fr

7

8   **Abstract**

9   Diffusive gradient in thin film (DGT) is used for aluminum monitoring in waters, where

10   content can reach more than 1 mg L^{-1}, but no information is available concerning its limit of linear

11   accumulation, leading to a risk of an underestimation of the water concentration. Furthermore, this

12   limit can be strongly affected by the pH due to changes of the aluminum speciation and global charge

13   of the binding phase. The linear accumulation capacities of three types of DGT, based on Chelex-100®

14   (DGT-Ch), titanium dioxide (DGT-Ti) and zirconium oxide (DGT-Zr), were determined as a function of

15   pH by time-series accumulation over 30 days. For DGT-Ch, it decreased with increasing pH: around 16

16   μg at pH 4.1, 5 μg at pH 5.3 and null at pH 8.6. The DGT-Ti and DGT-Zr had similar performances and

17   could accumulate aluminum over the whole tested pH range, but with a significantly higher limit of

18   linear accumulation at pH 8.6 (≈15 μg) compared to pH 4.1 (≈1 μg). The evolution of the accumulated

19   mass over time agreed with the predicted values except for DGT-Zr at pH 4.1 and 5.3, where a *ca.*

20   30% higher accumulation was observed. Application in natural freshwaters containing various

21   aluminum species and potential competitors confirmed the linear limits for the three types of DGT

22   and also the DGT-Zr tendency to over-estimate aluminum (up to 200% in some freshwater samples

23   compared to DGT-Ch and DGT-Ti). This phenomenon observed for DGT-Zr cannot be explained yet.

24   Currently, DGT-Zr is not recommended for aluminum monitoring.

25

I. INTRODUCTION

The presence of aluminum (Al) in freshwaters, varying from a few $\mu g\ L^{-1}$ to several $mg\ L^{-1}$ (Habs et al., 1997), is a major concern regarding its potential toxicity. Many studies have shown that it can have detrimental effects on aquatic organisms (Chassard-Bouchaud et al., 1992; Roy and Campbell, 1997). If freshwaters are used as drinking water resources without removal treatment, this element can also impact human health as it is considered as a risk factor for degenerative diseases (Exley, 2013). The environmental effects of Al are governed by its speciation rather than its total concentration. The speciation of Al mostly depends on pH (Harris et al., 1996). Acidic conditions lead to the presence of cationic species such as Al^{3+}, $AlOH^{2+}$ and $Al(OH)_2^+$ which, along with weak complexes (mainly inorganic), are generally recognized as the most reactive, and therefore the most bioavailable forms (Gensemer and Playle, 1999). In the pH range 6.0-7.5, Al is commonly precipitated as $Al(OH)_{3(s)}$ (Sposito, 1995). The anionic $Al(OH)_4^-$ form found in alkaline freshwaters is considered less toxic than cationic species but its toxicity mechanism is not clearly known (Wilson, 2011). It should be noted that the presence of ligands, such as dissolved organic matter, decreases the toxicity of Al (Roy and Campbell, 1997) by limiting its bioavailability. Therefore, the toxicity of Al in freshwaters varies with both pH and the presence of ligands such as organic matter (Sposito, 1995). A quantitative determination of the most reactive forms of Al is thus required for a relevant toxicity risk assessment.

The passive sampling by diffusive gradients in thin films (DGT), developed by Davison and Zhang (1994), is a suitable tool for speciation studies (Menegário et al., 2017; Zhang and Davison, 2015). The DGT samples only the labile fraction (*i.e.,* free element and fast-dissociating complexes) (Davison and Zhang, 2012), which is considered to be the most bioavailable, thus allowing a better assessment of the impacts on organisms (Røyset et al., 2005; Eismann et al., 2020). In addition, as an *in situ*

51 sampling technique, the DGT eliminates the issues associated to the sample storage by reducing the

52 risk of speciation change or contamination. Furthermore, this technique allows the determination of

53 time-weighted average concentrations and is thus more representative of organism's exposure than

54 concentrations determined from grab sampling (Allan et al., 2006), especially in dynamic systems

55 where the concentration and the speciation can vary over several hours.

56 When considering the different DGT configurations already available, various behaviors can be

57 expected for Al sampling. Several studies have shown that a conventional DGT device based on a

58 Chelex binding phase is able to sample Al, but only under acidic conditions (Panther et al., 2012;

59 Shiva et al., 2017). Another DGT, based on a titanium dioxide binding phase has also been used for Al

60 and allows its sampling under both acidic and alkaline conditions (Panther et al., 2012). It should be

61 noted that no information is yet available concerning the linear accumulation capacity of these two

62 binding phases for Al. However, this parameter is essential to ensure that there is no saturation, even

63 partial, of the binding phase which would induce an underestimation of the contamination. Such a

64 situation is particularly of concern in the case of waters with high labile Al content. It has been shown

65 that a DGT device based on a zirconium oxide binding phase has better binding capacities for several

66 oxyanions (Ding et al., 2016), but it has not been evaluated yet for Al sampling.

67 Furthermore, pH may strongly affect both the speciation of Al and the ionization state of binding

68 phase functions, consequently modifying the binding capacity. Indeed, according to pH, Al can be

69 positively charged (varying from +1 to +3), neutral or negatively charged (-1) *(Figure S1)*. Concerning

70 the binding phase, depending on the pH and its pH of zero-point charge (pH_{ZPC}), it can have a

71 negative, neutral or positive global charge *(Figure S1)*. These changes can lead to different binding

72 capacities: the amount of binding sites and / or the interactions between the Al species and the

73 binding phase can vary. The linear accumulation capacity of a binding phase shall thus be determined

74 considering the effect of pH.

75 In this paper, we propose an in-depth study of the accumulation capacities of DGT for Al to take

76 full advantage of its time integrative capacities in natural waters. The objectives of this work are to

determine the limits of linear accumulation of three binding phases (Chelex, titanium dioxide or zirconium oxide) considering the effect of pH and to evaluate the DGT based on a zirconium oxide binding phase as an alternative for Al sampling in freshwaters.

II. MATERIALS AND METHODS

II.1. MATERIALS, REAGENTS AND SOLUTIONS

All reagents were analytical grade or higher. Ultrapure water (Milli-Q system, water resistivity > 18.2 MΩ.cm) was used to prepare all the solutions. All the reusable materials, including the DGT devices, were cleaned by immersion in a 10% (V/V) HNO_3 bath for 24 h then rinsed with ultrapure water prior to use. A 1000 mg L^{-1} Al stock solution was prepared from $Al(NO_3)_3.9H_2O$ (Honeywell Fluka, ACS quality).

II.2. DGT PROCEDURES

II.2.1. DGT SAMPLERS

Three DGT binding gels were studied: Chelex-100® (iminodiacetic functions), Metsorb® (titanium dioxide) and zirconium oxide. The Chelex and titanium dioxide binding gels were purchased from DGT Research Ltd. The zirconium oxide binding gels were prepared according to the protocol used by Devillers et al. (2017). The DGT devices were assembled using plastic holders (DGT Research Ltd.) enclosing a binding gel, a polyacrylamide diffusive gel (0.78 mm thick, DGT Research Ltd.) and a polycarbonate filter membrane (0.4 µm pore diameter, 0.01 mm thick, Whatman). The corresponding DGT devices were labelled DGT-Ch, DGT-Ti and DGT-Zr.

II.2.2. ELUTION

After exposition, the DGT were dismantled and the binding gels were eluted during 24 h at 21 ± 1 °C in a temperature controlled room. The elution step was performed using 1 mL of 1 mol L^{-1} HNO_3 for the Chelex binding gels (Warnken et al., 2007), 1 mL of 0.1 mol. L^{-1} NaOH for the titanium

100   dioxide binding gels and 2 mL of 0.2 mol L^{-1} NaOH for the zirconium oxide binding gels. The protocol

101   for the titanium dioxide binding gels was adapted from Bennett et al. (2010) by decreasing the NaOH

102   concentration by ten times to avoid matrix effect caused by sodium during Al analysis by atomic

103   absorption spectrometry. The protocol for the zirconium oxide binding gels was adapted from Ding

104   et al. (2016) by removing H_2O_2 to avoid apparition of zirconium oxide precipitates in the eluate over

105   time, as highlighted in their publication.

106   An elution yield of 0.84 was used for the Chelex binding gels according to Panther et al.

107   (2012) and Devillers et al. (2017). The elution yield for the titanium and zirconium oxide binding gels

108   were determined since the protocols were adapted from Bennett et al. (2010) and Ding et al. (2016),

109   respectively. For this purpose, binding gels were directly immersed in 9 mL of 10^{-2} mol L^{-1} NaNO₃

110   solution containing 50 µg L^{-1} of Al at pH 4.0 or 8.5 (triplicates for titanium dioxide and six replicates

111   for zirconium oxide). The pH was adjusted using 1 mol L^{-1} HNO₃ and NaOH, with addition of 5.10^{-3}

112   mol L^{-1} Na₂CO₃ for pH 8.5. After 24 h, the gels were recovered and eluted prior analysis. Samples of

113   each exposure solution were taken before and after gel immersion to determine the accumulated

114   mass of Al in each binding gel. The elution yield was calculated as the ratio between the eluted mass

115   and the accumulated mass.

116   II.2.3.   DGT BLANKS

117   As Al is a ubiquitous element, the device contamination level was measured for each type of

118   DGT. For this purpose, triplicates of unexposed DGT devices were assembled, dismantled, and eluted

119   with the same procedure than applied to the exposed DGT.

120   II.3. PH INFLUENCE ON TIME-SERIES ACCUMULATION

121   To study the influence of pH only on the linear accumulation capacities, time-series

122   accumulation were performed in NaNO₃ solutions in absence of competitors. pH values close to the

123   neutrality (pH 6.0 to 7.5) could not be studied in laboratory because of the precipitation of Al,

124   impeding having a quantifiable and stable concentration. The time-series accumulation of Al by DGT

125   were consequently studied at pH 4.1, 5.3 and 8.6. These three pH allowed covering the main range of

126   dissolved inorganic Al species present in aquatic systems *(Figure S1)*. To guarantee the Al

127   concentrations in the exposure solutions, they were set to the highest possible value preventing the

128   formation of insoluble $Al(OH)_{3(s)}$, for each studied pH. The corresponding concentrations were 45, 17

129   and 85 µg L^{-1} for pH 4.1, 5.3 and 8.6, respectively. The ionic strength of these solutions was imposed

130   using 10^{-2} mol L^{-1} $NaNO_3$ and the pH was adjusted using 1 mol L^{-1} HNO_3 and NaOH, with addition of

131   5.10^{-3} mol L^{-1} Na_2CO_3 for pH 8.6. Before starting the experiments, the solutions were left to

132   equilibrate for at least 72 h.

133   For each pH, DGT-Ch, DGT-Ti and DGT-Zr were deployed in a well-stirred solution at 20 ± 1 °C

134   using 20 L polyethylene containers (up to 24 DGT per container). The accumulation of Al was

135   evaluated over eight deployment times between 4 h and 30 days, with triplicates for each duration.

136   The pH was monitored daily and the solutions were sampled at each DGT deployment and removal

137   (or daily if no device was added/retrieved) to monitor Al concentration.

138   **II.4. DGT DEPLOYMENT IN NATURAL WATERS**

139   DGT deployments were performed in natural waters to confirm both the linear accumulation

140   capacity and the accumulation behavior of the three studied binding phases obtained in $NaNO_3$

141   solutions. For this purpose, three natural waters were selected for their significant dissolved Al

142   concentrations (between 100 and 300 µg L^{-1}) and their pH (between 5 and 7) covering a large part of

143   the environmental range *(Table 1)*. They correspond to a subsurface runoff used for drinking water

144   purpose (water C) and two rivers from headwaters located in the North-West of the Massif Central in

145   France (water M and R). More details about their physicochemical composition can be found in

146   *Table S1*.

147

Table 1 : Main characteristics of the natural waters studied. (Mean ± SD, n ≥ 3, DOC: Dissolved Organic Carbon)

	pH	Conductivity ($\mu S\ cm^{-1}$)	Dissolved Al ($\mu g\ L^{-1}$)	DOC ($mg\ L^{-1}$)
Water C	5.0 ± 0.2	26 ± 2	290 ± 40	1.0 ± 0.7
Water M	6.0 ± 0.1	27 ± 2	97 ± 5	8 ± 1
Water R	7.1 ± 0.1	163 ± 3	260 ± 50	9 ± 4

Preliminary experiments showed that only DGT deployments in water C would allow to get close to the limits of linear accumulation of the studied DGT in an acceptable deployment time (*i.e.* < 2 weeks to avoid major changes in water composition). Only this natural water was therefore used to verify that the linear accumulation capacities determined in synthetic solutions are still valid in natural waters. DGT-Ch, DGT-Ti and DGT-Zr were thus deployed in triplicates in water C for two durations (4 h and 40 h) to guarantee the absence of saturation by comparing the results of short and long deployments. The longer deployment time was estimated according to ***Equation 1*** from the dissolved Al concentration to get close to the limit of linear accumulation obtained in the $NaNO_3$ solution at pH 5.3.

In addition to the water C, the natural waters M and R were used to compare the behavior of each type of DGT in a non-saturating condition. The duration of deployment, set to stay far below the beginning of saturation of the binding gels, was chosen based on the results obtained in $NaNO_3$ solutions and according to the DGT-available Al content of each water (estimated during preliminary experiments). DGT were thus deployed during 3 days in water M and 7 days in water R.

To control as much as possible the conditions during DGT deployment, the experiments were performed in the lab directly after sampling the natural waters. DGT-Ch, DGT-Ti and DGT-Zr were deployed in 5 L (for water C and M) or 20 L (for water R) of well-stirred solution in polyethylene containers. The exposition temperature was set to 6 ± 1 °C (controlled by Tinytag temperature loggers) to remain close to the field conditions (waters were sampled in winter 2021). During DGT

169   exposure, the pH and Al concentration were monitored daily. The dissolved Al concentration was

170   determined after filtration at 0.2 µm (cellulose acetate, Sartorius). In addition, ultrafiltration with a

171   low cutoff membrane (3 kDa, Vivaspin) was performed to separate large complexes from "free" Al

172   and/or small complexes. The ultrafiltration was carried out by centrifugation of 5 mL of natural

173   waters at 6000 g for 10 min at 6 ± 1 °C. Filters and ultrafilters were systematically pre-conditioned

174   with 5 mL of the solution to be filtered to avoid Al sorption or release.

175   **II.5. ALUMINUM MEASUREMENTS**

176   II.5.1. ANALYSIS

177   The eluates and exposure solutions were analyzed by atomic absorption spectrometry with

178   electrothermic atomization (ET-AAS, Agilent 240 Z) using a platform graphite tube. A modifier

179   consisting in 0.64 mg L^{-1} (final concentration) of NH_4NO_3 and $Ca(NO_3)_2$ was used. All samples and

180   standards were acidified at 1% (V/V) with HNO_3. The standard addition method was applied to

181   eluates of DGT exposed in natural waters to detect any potential matrix effects. For quality

182   assurance, blanks (HNO_3 1% V/V) and a control solution (20 µg L^{-1}, prepared daily) were analyzed

183   every ten samples. In addition, a 20 µg L^{-1} laboratory certified solution was analyzed at the beginning

184   and the end of each sequence (recovery > 95%). The limit of quantification of the method (according

185   to IUPAC) was estimated at 5 µg L^{-1}.

186   II.5.2. C$_{DGT}$ DETERMINATION

187   The concentration estimated by DGT, C$_{DGT}$ (µg L^{-1}), was calculated using **Equation 1** (Davison

188   and Zhang, 1994):

189   $C_{DGT} = \frac{m\Delta_g}{DAt}$ **Equation 1**

190   where m (ng) is the mass of Al accumulated in the binding phase, Δg is the thickness of the diffusive

191   layer (0.079 cm), t (s) is the exposure duration, A is the exposure area to solution (3.14 cm²) and

192   D (cm² s^{-1}) is the diffusion coefficient of Al. The values of D were taken from the literature (Panther et

193 al., 2012; Shiva et al., 2017) according to the pH of the solution and corrected according to the

194 average temperature during the deployment using the Stokes-Einstein relationship (values are listed

195 in *Table S2)*.

196   II.5.3. SPECIATION CALCULATION AND STATISTICS

197   Visual MINTEQ 3.1 software was used with the default database constants to determine the

198 speciation of Al according to pH, considering $Al(OH)_{3(s)}$ as the dominant solid phase (log K = 10.8) and

199 equilibrium with atmospheric CO_2. The Stockholm Humic Model (SHM) was used to simulate Al

200 interactions with organic matter in natural waters.

201   For experiments in natural waters, statistical analyses were performed to compare the results

202 obtained by each type of DGT. ANOVA tests were used to verify the equality of the means and

203 completed, if necessary, by a Student LSD (least significant difference) test to identify the different

204 means. All tests were conducted with a statistical significance level of p = 0.05. In addition, for

205 experiments in water C, the uncertainty of the ratios between the C_{DGT} obtained for 40 h and 4 h

206 deployment was calculated by propagation of uncertainty.

207

III. RESULTS AND DISCUSSION

208

III.1.   ELUTION

209

III.1.1. BLANK CONTAMINATION

210

211   The eluates of unexposed DGT revealed a rather low and constant contamination

212 (0.024 ± 0.004 µg, 0.032 ± 0.001 µg and 0.040 ± 0.004 µg per binding gel for DGT-Ch, DGT-Ti and

213 DGT-Zr, respectively). The mean DGT blank value was consequently systematically subtracted to the

214 results of each exposed DGT.

III.1.2. ELUTION YIELDS

216	There was no difference between the elution yields determined at pH 4.0 and 8.6. Values of

217	0.66 ± 0.03 (n = 12) and 0.65 ± 0.02 (n = 6) were obtained for the zirconium oxide and titanium

218	dioxide binding gels respectively. For the titanium dioxide binding gels, the elution yield obtained

219	with 0.1 mol L^{-1} NaOH was 17% lower than with 1 mol L^{-1} NaOH (Panther et al., 2012). However, this

220	adapted elution protocol allows analyzing undiluted eluates without suffering any matrix effect from

221	NaOH. In the end, it allows decreasing the quantification limit to around an accumulated mass of

222	10 ng, by avoiding the systematic ten times dilution of the original procedure.

223

224	**III.2. DGT LINEAR ACCUMULATION CAPACITIES**

225	III.2.1. TIME-SERIES ACCUMULATION IN NaNO$_3$ SOLUTIONS

226	To determine the linear accumulation capacities of each type of DGT according to pH only, the

227	accumulation of Al species by DGT-Ch, DGT-Ti and DGT-Zr was investigated in controlled NaNO$_3$

228	solutions at pH 4.1 ± 0.1, 5.3 ± 0.1 and 8.6 ± 0.1. Note that to avoid Al precipitation and thus control

229	the concentration of "DGT available Al", the pH range 6.0 to 7.5 was not considered. The Al

230	speciation as a function of pH, determined using Visual MINTEQ, is given in **Table 2**. The studied

231	range of pH allowed investigating the accumulation of both cationic and anionic species.

232	The Al concentration remained stable throughout the DGT deployment, with variations lower

233	than 5%. Consequently, the DGT exposure concentration (C) used for the calculation was the mean

234	concentration of samples taken over time. The accumulated mass m (µg) was plotted as a function of

235	the deployment duration, t (day) **(Figure 1)**. According to **Equation 1**, the plot of m *versus* t should

236	be linear, with CDA/Δg as slope, up to the beginning of the saturation of the binding phase.

237	Therefore, for each type of DGT, the linear accumulation capacity can be determined as the m value

238	associated to the linearity disruption. Given the uncertainty between the DGT triplicates (RSD

239 generally lower than 10%), the accumulation linearity was considered lost when a difference higher

240 than 10% was observed between the measured and the extrapolated linear value. In addition, the

241 predicted accumulation was determined using *Equation 1* (diffusion coefficients were taken from

242 literature according to the pH, *Table S2*) to assess the compliance of the linear accumulation with the

243 DGT theory*.*

244 **Table 2: Aluminum speciation according to pH in NaNO$_3$ solutions, determined by Visual MINTEQ.**

pH	[Al] (μg L^{-1})	% of Al species				
		Al^{3+}	AlOH^{2+}	Al(OH)$_2$$^+$	Al(OH)$_{3(aq)}$	Al(OH)$_4$$^-$
4.1 ± 0.1	45	94.7	5.2	0.1	-	-
5.3 ± 0.1	17	44.0	38.1	16.9	0.9	0.1
8.6 ± 0.1	85	-	-	-	0.5	99.5

245

246 At pH 4.1 *(Figure 1, a)*, a linear and theoretically predictable accumulation was obtained with

247 DGT-Ch up to 30 days. The mean accumulated mass of 15.9 μg obtained is 10% lower than the

248 predicted one, suggesting a beginning of saturation, but staying in the limit of the accepted

249 deviation. The limit of linear accumulation of the DGT-Ch is thus probably around 16 μg. With DGT-Ti

250 and DGT-Zr, a linear accumulation was observed for 2 days only, up to a mass of 1.11 ± 0.07 μg and

251 1.3 ± 0.1 μg respectively. The experimental accumulation on DGT-Ti followed the predicted trend,

252 but a surprisingly higher accumulated mass was observed with the DGT-Zr (33% slope offset

253 compared to prediction).

254 At pH 5.3 *(Figure 1, b)*, the DGT-Ch and DGT-Ti had the same behavior, with a linear and

255 theoretically predictable accumulation up to 20 days (accumulated mass of 4.0 ± 0.2 μg and

256 4.6 ± 0.3 μg respectively). The mean accumulated mass for 30 days of exposition was 10% lower than

257 the linear part, suggesting a potential beginning of saturation of both binding phases. The linear

258 accumulation capacity of DGT-Ch and DGT-Ti can thus be estimated around 5 μg. DGT-Zr showed a

259 slightly different behavior. Its accumulation was also linear, but the saturation did not seem to be

260   reached over the 30 days of exposition (linear accumulation up to 8.1 ± 0.8 µg). However, it should

261   be noted that the accumulation was slightly higher than the prediction (23% deviation between

262   experimental and predicted slope).

263   At pH 8.6 *(Figure 1, c)*, the DGT-Ch showed a very low accumulation. These results are in

264   agreement with Panther et al. (2012) who have already observed an under-accumulation above pH

265   7.5 with this setup. The DGT-Ti and DGT-Zr presented the same behavior with a linear accumulation,

266   consistent with the theory, up to 10 days, corresponding to an accumulated mass of 11.6 µg. The

267   mass of 17 µg obtained after 17 days of exposition being 15% lower than the linear part, the limit of

268   linear accumulation of DGT-Ti and DGT-Zr is thus between 11 and 17 µg. At this pH, no higher

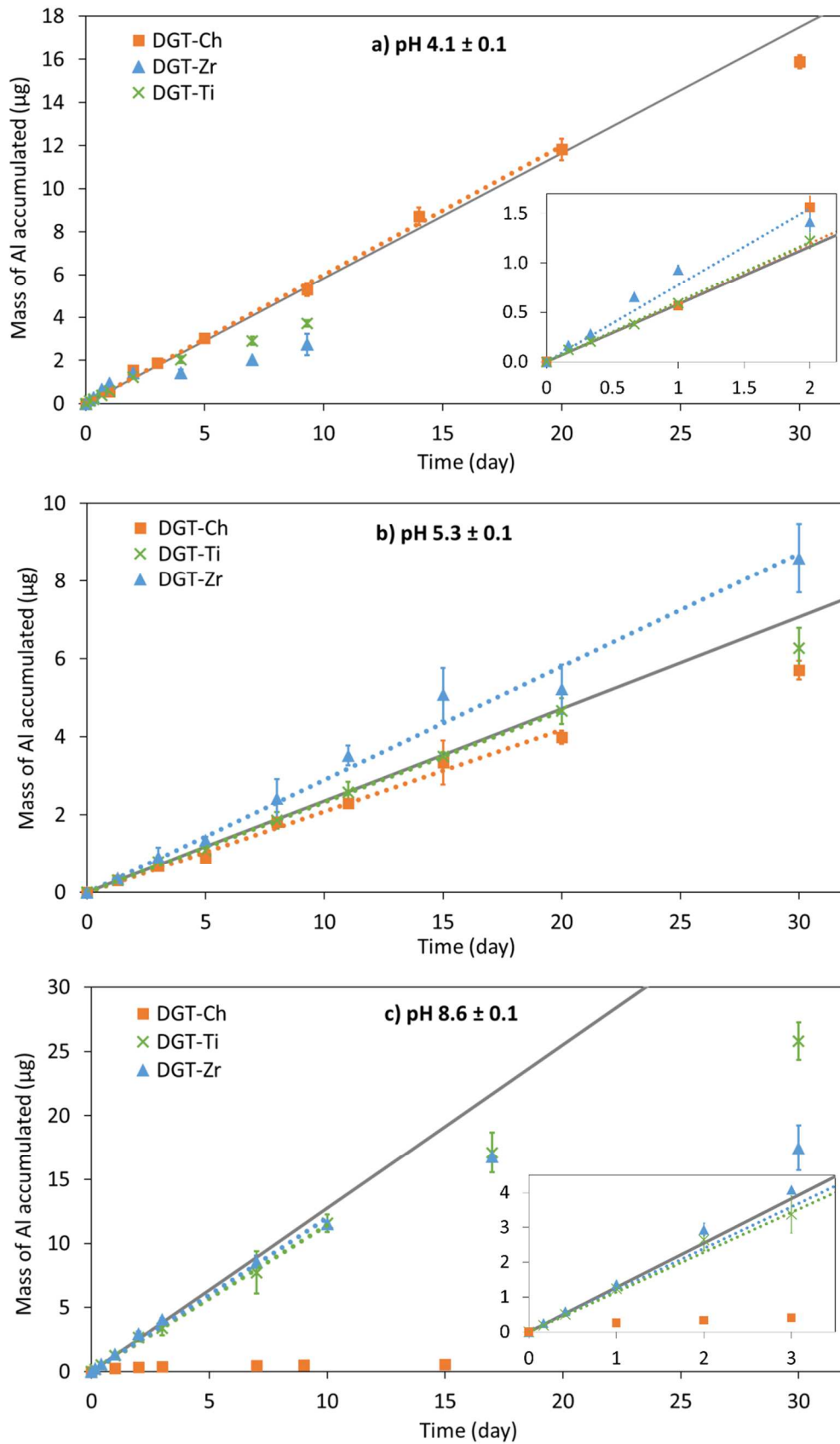269   accumulation compared to the prediction was observed for DGT-Zr.

Figure 1: Accumulated mass of Al as a function of time at pH 4.1 ± 0.1 (a); 5.3 ± 0.1 (b) and 8.6 ± 0.1 (c) (mean ± SD, n = 3, grey line: predicted accumulation using Equation 1, dotted lines: linear accumulation).

270

271   These results show that the DGT-Ch cannot be used at pH 8.6 but offers the highest linear

272   accumulation capacity at pH 4.1. The DGT-Ti and DGT-Zr can accumulate Al over the whole tested pH

273   range, with a higher linear accumulation capacity at pH 8.6. The effect of pH on both Al speciation

274   and binding phase's charge could explain the differences in accumulation capacities *(Figure S1)*.

275   Indeed, Al species and the binding phase having charges of the same sign would generate

276   electrostatic repulsions, potentially resulting in a decreased accumulation capacity. In the case of the

277   Chelex binding gel, the speciation of the chelating iminodiacetic functions leads to an overall

278   negative charge above pH 6. At pH 4.1, Al is almost totally under the most positively charged species:

279   Al^{3+} *(Table 2)*. It has already been demonstrated that Chelex-100 is the binding phase of choice for

280   accumulating trivalent cations (Warnken et al., 2009; Zhang and Davison, 1995). However, at pH 8.6,

281   the dissolved Al is almost totally present as the anionic form $Al(OH)_4^-$ *(Table 2)* and the DGT-Ch is

282   negatively charged. Thus, Al is hardly accumulated probably due to electrostatic repulsions.

283   The charge of the titanium dioxide and zirconium oxide binding gel can be determined from

284   their pH_{ZPC} *(Figure S1)*. With a pH_{zpc} of 5.9 (Kosmulski, 2002a), the titanium dioxide is overall

285   positively charged below pH 5.9 and negatively charged above. In the literature, the pH_{ZPC} of

286   zirconium (hydr)oxide is given from 4 to 8.6, with an average and median values at 6.5 (Kosmulski,

287   2002b). Due to the different structures of the zirconium oxides, the concept of one recommended

288   pH_{ZPC} does not work particularly well (Kosmulski, 2002b). Thus, to estimate the charge of the

289   zirconium oxide phase used in our study, measurements of the zeta potential as a function of pH

290   have been performed and a pH_{ZPC} of 5.5 was determined (the procedure and values are detailed in

291   *Figure S2*). This value is in a close range of the median value proposed by Kosmulski (2002b).

292   According to our results, at pH 4.1, the DGT-Ti and DGT-Zr have a linear accumulation capacity at

293   least eight times lower than the DGT-Ch. At this pH, these two sorbents are positively charged, like

294   Al. Thus, the lowered capacity could be due to electrostatic repulsions. At pH 5.3, it clearly appears

295   that DGT-Ti and DGT-Zr have a higher linear accumulation capacity (at least 4 times higher) compared

296   to pH 4.1. At this pH, the dissolved Al species are still mostly positively charged *(Table 2)* but the two

297 sorbents are nearly neutral, therefore strongly reducing the electrostatic repulsions and thus

298 resulting in an increased accumulation capacity. However, at pH 8.6, whereas DGT-Ti, DGT-Zr and Al

299 are negatively charged, significantly higher linear accumulation capacities were determined. This

300 observation is consistent with reports of oxyanions sorption by these phases in the literature (Ding et

301 al., 2016), meaning that the potential electrostatic repulsions do not seem to significantly reduce the

302 accumulation capacity compared to pH 5.3. It should be noted that DGT-Zr was shown to accumulate

303 a higher mass of Al compared to the prediction at pH 4.1 and 5.3 but at this stage, there is no clear

304 explanation.

305 ### III.2.1. EXPERIMENTS IN A NATURAL WATER

306 DGT deployments were performed in the natural water C to check that the limits of linear

307 accumulation determined in $NaNO_3$ solutions are also valid in environmental conditions. Indeed,

308 compared to the $NaNO_3$ solutions used, a freshwater represents a complex matrix, with a more

309 complex speciation of Al and the presence of competitors (*e.g.* Fe, Mn, Ca, see **Table S1**) for sites

310 onto DGT binding phase. The selected freshwater has a high DGT available Al concentration that

311 allows reaching a potential saturation of the binding phases in a short duration. Two deployment

312 durations (4 h and 40 h) were compared to verify the absence of saturation.

313 For the short deployment time (4 h), the accumulated masses were lower than 1 µg, ensuring no

314 risk of saturation. After 40 h exposition, as expected, the accumulated masses (3.2 ± 0.8, 4.5 ± 0.3

315 and 4.1 ± 0.8 µg for DGT-Ch, DGT-Ti and DGT-Zr respectively) were close to the linear accumulation

316 capacity previously determined in $NaNO_3$ at a similar pH (≈5 µg at pH 5.3). The corresponding C_{DGT}

317 value were then calculated for each deployment duration according to **Equation 1**. In case of

318 saturation, even partial, the C_{DGT} values obtained from the 40 h exposed DGT should be significantly

319 lower than the one obtained for 4 h. The ratios between C_{DGT} obtained with 40 h deployment and 4 h

320 deployment were 1.19 ± 0.24, 1.02 ± 0.08 and 0.95 ± 0.20 for DGT-Ch, DGT-Ti and DGT-Zr,

321 respectively. These ratios are not statistically different from 1, which means that no significant

15

322 difference can be found between the short and long deployment duration. It can thus be concluded

323 that none of the three binding phases was saturated when accumulating ~4 µg of Al. Consequently,

324 the linear accumulation capacities determined in the NaNO$_3$ solution appear to remain valid in this

325 type of natural water, with a more complex Al speciation and potential competitors.

326   This application in water C also highlights the importance of knowing the limit of linear

327 accumulation of DGT to properly set the deployment duration. Indeed, in this case of highly

328 contaminated water by Al, it can be nearly reached within two days of deployment, considerably

329 reducing the duration of the monitoring and the DGT time integrative capacity (which is typically

330 1 or 2 weeks).

331

III.3.   COMPARISON OF BINDING PHASES BEHAVIORS IN NATURAL WATERS

332

333   To confirm the accumulation behaviors observed in NaNO$_3$ solutions, additional experiments

334 were performed using natural waters (waters C, M and R) with high dissolved Al concentrations, and

335 presence of organic matter *(Table 1)*. To correctly compare the accumulation by each type of DGT,

336 these experiments needed to be performed in non-saturating conditions. This condition has already

337 been confirmed for experiments in the water C. For the waters M and R, the accumulated Al masses

338 were all lower than 1.2 µg *(Table S3)* and thus far below the estimated linear accumulation capacities

339 as expected. These accumulated masses were used to calculate C$_{DGT}$ according to *Equation 1* and

340 using diffusion coefficients selected from literature *(Table S2)*. The corresponding results are

341 presented in *Figure 2* with the Al concentrations determined in the natural waters after filtration

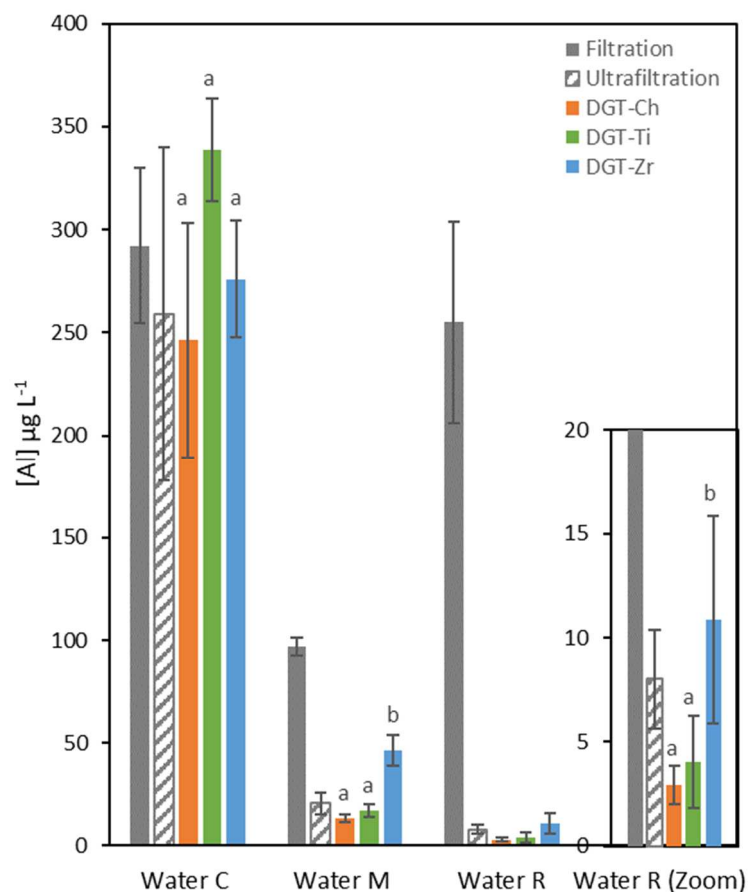342 ("dissolved" Al) and ultrafiltration ("truly dissolved" Al).

Figure 2: Concentration of Al obtained by filtration, ultrafiltration and DGT in natural waters (mean ± SD, n ≥ 2)**.** For each water, the means obtained by DGT with the same letter are statistically not different.

343   In each water, the C_{DGT} obtained with DGT-Ch and DGT-Ti were in agreement, as previously

344   observed in $NaNO_3$ solutions at pH 4.1 and 5.3. This seems to confirm their similar accumulation

345   behavior of Al species between pH 4.1 and 7.1, even in the presence of organic matter. The DGT-Zr

346   had the same accumulation behavior than DGT-Ch and DGT-Ti in the water C but led to significantly

347   higher (about two times) accumulations in the waters M and R. After exposure in these two waters, a

348   systematic orange coloration of the zirconium oxide binding gels was observed *(Figure S3)*, indicating

349   a potential accumulation of other compounds. The hypothesis that these compounds may induce

350   matrix effects during the analysis was tested and discarded by performing standard addition

351   quantifications. The significant presence of iron in waters M and R compared to water C *(Table S1)*,

352   where this phenomenon was not observed, was also suspected to induce the coloration. The

353   zirconium oxide binding gels could have accumulated iron oxyhydroxides, known to be brown-

354   orange. After elution, the gels became colorless *(Figure S3)*, suggesting the potential transfer of iron

355   into the eluate. However, analysis of the eluates did not reveal any significant presence of iron. This

356   hypothesis was thus discarded. Another hypothesis could be the accumulation of other Al species by

357   the zirconium oxide binding gel (*e.g.* complexes with organic matter). For the waters M and R, the

358   ultra-filtered concentration was considerably lower than the filtered concentration *(Figure 2)*,

359   indicating that most part of the dissolved Al was probably present as large-size complexes. This

360   observation can be consistent with the presence of significant organic matter in these waters *(Table*

361   *1)*. In the water C with a low content of organic matter *(Table 1)*, there was no significant difference

362   between the filtered and ultrafiltered concentrations *(Figure 2)*, suggesting that all the aluminum

363   was "truly dissolved". Thus, the Al complexes with organic matter are probably more present in the

364   waters M and R than in the water C. These observations are consistent with the Al speciation

365   predicted by Visual MINTEQ which shows that more than 90% of Al would be bound to organic

366   matter in waters M and R against only 25% in water C. The Al complexes with organic matter could

367   perhaps be partly accumulated by the DGT-Zr, resulting in a higher accumulation compared to DGT-

368   Ch and DGT-Ti in waters M and R.

369   **III.4.   GENERAL EVALUATION OF DGT-ZR**

370   This work evaluates for the first time the DGT-Zr as an alternative for the sampling of Al. The

371   experiments revealed that the DGT-Zr could sample both cationic and anionic Al species from pH 4.1

372   to 8.6. However, in contrast to the higher capacities reported in the literature for other oxyanions

373   (Ding et al., 2016), no higher linear accumulation capacity has been observed for Al in the tested

374   conditions. In addition, compared to DGT-Ch and DGT-Ti, the use of DGT-Zr induces an over-

375   estimation of Al concentration in both $NaNO_3$ solutions and natural waters. Indeed, a ~30% higher

376   accumulation compared to the predicted value was observed in $NaNO_3$ solutions at pH 4.1 and 5.3.

377   DGT-Zr had a similarly behavior to DGT-Ch and DGT-Ti in one of the studied natural water but it

378   accumulated up to 200% more Al in the others. The potential accumulation of some organic Al

379   species by only the DGT-Zr could be assumed in the natural waters but would not explain the higher

380   accumulation observed in $NaNO_3$ solutions. This phenomenon observed in both synthetic and natural

381   waters for DGT-Zr cannot be explained yet. Consequently, this setup is not recommended for Al

382   monitoring without further investigations.

IV. CONCLUSION

384   By impacting both the Al speciation and the global charge of the binding phase, the pH strongly

385   affects the binding capacities of DGT. The linear accumulation capacities of DGT-Ch, DGT-Ti and DGT-

386   Zr vary up to a factor ten (from ≈1 µg to ≈15 µg) between pH 4.1 and 8.6. These capacities can easily

387   be reached within few tens of hours field deployment in freshwaters with high Al concentrations.

388   This parameter must therefore be cautiously considered to avoid DGT saturation. In contrast to what

389   could be expected, DGT-Zr did not offer higher capacity compared to DGT-Ti and, surprisingly,

390   induces an over-estimation of Al concentration in water. Consequently, the DGT-Zr is not currently

391   recommended for Al sampling.

392   Based on our results, it appears that DGT-Ti should be used for pH > 7 since DGT-Ch shows poor

393   accumulation. DGT-Ch and DGT-Ti can both be used for Al sampling at pH ≤ 7 as they present relative

394   similar accumulation behaviors in this pH range. However, the DGT-Ch should be preferred for

395   pH ≤ 5.3 and the DGT-Ti seems more suitable for pH > 5.3 because of their respective higher linear

396   accumulation capacity. The higher capacity will allow longer deployments and consequently a better

397   temporal integration of the Al contamination without the risk of DGT saturation.

398

402

406

References

Allan, I.J., Vrana, B., Greenwood, R., Mills, G.A., Roig, B., Gonzalez, C., 2006. A "toolbox" for biological and chemical monitoring requirements for the European Union's Water Framework Directive. Talanta 69, 302–322. https://doi.org/10.1016/j.talanta.2005.09.043

Bennett, W., R Teasdale, P., Panther, J., Welsh, D., Jolley, D., 2010. New Diffusive Gradients in a Thin Film Technique for Measuring Inorganic Arsenic and Selenium(IV) Using a Titanium Dioxide Based Adsorbent. Analytical chemistry 82, 7401–7. https://doi.org/10.1021/ac101543p

Chassard-Bouchaud, C., Galle, Ch., Lopez-Rabereau, E., 1992. Bioaccumulation d'aluminium chez la truite Salmo truffa fario soumise au retombées des pluies acides : étude structurale, ultrastructurale et microanalytique. Revue des sciences de l'eau 5, 37. https://doi.org/10.7202/705119ar

Davison, W., Zhang, H., 2012. Progress in understanding the use of diffusive gradients in thin films (DGT) back to basics. Environmental Chemistry 9, 1–13. https://doi.org/10.1071/EN11084

Davison, W., Zhang, H., 1994. In situ speciation measurements of trace components in natural waters using thin-film gels. Nature 367, 546–548. https://doi.org/10.1038/367546a0

Devillers, D., Buzier, R., Charriau, A., Guibaud, G., 2017. Improving elution strategies for Chelex®-DGT passive samplers. Anal Bioanal Chem 409, 7183–7189. https://doi.org/10.1007/s00216-017-0680-4

Ding, S., Xu, D., Wang, Yanping, Wang, Yan, Li, Y., Gong, M., Zhang, C., 2016. Simultaneous Measurements of Eight Oxyanions Using High-Capacity Diffusive Gradients in Thin Films (Zr-Oxide DGT) with a High-Efficiency Elution Procedure. Environ. Sci. Technol. 50, 7572–7580. https://doi.org/10.1021/acs.est.6b00206

Eismann, C.E., Menegário, A.A., Gemeiner, H., Williams, P.N., 2020. Predicting Trace Metal Exposure in Aquatic Ecosystems: Evaluating DGT as a Biomonitoring Tool. Expo Health 12, 19–31. https://doi.org/10.1007/s12403-018-0280-3

Exley, C., 2013. Human exposure to aluminium. Environ. Sci.: Processes Impacts 15, 1807–1816. https://doi.org/10.1039/C3EM00374D

Gensemer, R.W., Playle, R.C., 1999. The Bioavailability and Toxicity of Aluminum in Aquatic Environments. Critical Reviews in Environmental Science and Technology 29, 315–450. https://doi.org/10.1080/10643389991259245

Habs, H., International Programme on Chemical Safety, Weltgesundheitsorganisation (Eds.), 1997. Aluminium, Environmental health criteria. World Health Organization, Geneva.

Harris, W.R., Berthon, G., Day, J.P., Exley, C., Flaten, T.P., Forbes, W.F., Kiss, T., Orvig, C., Zatta, P.F., 1996. Speciation of aluminum in biological systems. Journal of Toxicology and Environmental Health 48, 543–568. https://doi.org/10.1080/009841096161069

Kosmulski, M, 2002(a). The significance of the difference in the point of zero charge between rutile and anatase. Advances in Colloid and Interface Science 99, 255–264. https://doi.org/10.1016/S0001-8686(02)00080-5

Kosmulski, M., 2002(b). The significance of the points of zero charge of zirconium (hydr)oxide reported in the literature. Journal of Dispersion Science and Technology 23, 529–538. https://doi.org/10.1081/DIS-120014021

448 Menegário, A.A., Yabuki, L.N.M., Luko, K.S., Williams, P.N., Blackburn, D.M., 2017. Use of diffusive
449   gradient in thin films for in situ measurements: A review on the progress in chemical
450   fractionation, speciation and bioavailability of metals in waters. Analytica Chimica Acta 983,
451   54–66. https://doi.org/10.1016/j.aca.2017.06.041
452 Panther, J.G., Bennett, W.W., Teasdale, P.R., Welsh, D.T., Zhao, H., 2012. DGT measurement of
453   dissolved aluminum species in waters: Comparing chelex-100 and titanium dioxide-based
454   adsorbents.   Environmental   Science   and   Technology   46,   2267–2275.
455   https://doi.org/10.1021/es203674n
456 Roy, R.L., Campbell, P.G.C., 1997. Decreased toxicity of Al to juvenile atlantic salmon (Salmo salar) in
457   acidic soft water containing natural organic matter: A test of the free-ion model.
458   Environmental Toxicology and Chemistry 16, 1962–1969. https://doi.org/10.1897/1551-
459   5028(1997)016<1962:DTOATJ>2.3.CO;2
460 Røyset, O., Rosseland, B.O., Kristensen, T., Kroglund, F., Garmo, Ø.A., Steinnes, E., 2005. Diffusive
461   gradients in thin films sampler predicts stress in brown trout (Salmo trutta L.) exposed to
462   aluminum in acid fresh waters. Environmental Science and Technology 39, 1167–1174.
463   https://doi.org/10.1021/es049538l
464 Shiva, A.H., Teasdale, P.R., Welsh, D.T., Bennett, W.W., 2017. Evaluation of the DGT technique for
465   selective measurement of aluminium and trace metal concentrations in an acid drainage-
466   impacted coastal waterway. Environmental Science: Processes and Impacts 19, 742–751.
467   https://doi.org/10.1039/c6em00276e
468 Sposito, G., 1995. The Environmental Chemistry of Aluminum, Second Edition. CRC Press.
469 Warnken, K.W., Davison, W., Zhang, H., Galceran, J., Puy, J., 2007. In situ measurements of metal
470   complex exchange kinetics in freshwater. Environmental Science and Technology 41, 3179–
471   3185. https://doi.org/10.1021/es062474p
472 Warnken, K.W., Lawlor, A.J., Lofts, S., Tipping, E., Davison, W., Zhang, H., 2009. In situ speciation
473   measurements of trace metals in headwater streams. Environmental Science and Technology
474   43, 7230–7236. https://doi.org/10.1021/es900112w
475 Wilson, R.W., 2011. 2 - Aluminum, in: Wood, C.M., Farrell, A.P., Brauner, C.J. (Eds.), Fish Physiology,
476   Homeostasis and Toxicology of Non-Essential Metals. Academic Press, pp. 67–123.
477   https://doi.org/10.1016/S1546-5098(11)31024-2
478 Zhang, H., Davison, W., 2015. Use of diffusive gradients in thin-films for studies of chemical
479   speciation   and   bioavailability.   Environmental   Chemistry   12,   85-.
480   https://doi.org/10.1071/en14105
481 Zhang, H., Davison, W., 1995. Performance Characteristics of Diffusion Gradients in Thin Films for the
482   in Situ Measurement of Trace Metals in Aqueous Solution. Analytical Chemistry 67, 3391–
483   3400. https://doi.org/10.1021/ac00115a005
484